

MRI in Patients with Implantable Devices: A Numerical Model for the Evaluation of Lead Heating

E Mattei, M Triventi, G Calcagnini, F Censi, P Bartolini

Italian National Institute of Health, Rome, Italy

Abstract

The radiofrequency (RF) field used in Magnetic Resonance Imaging (MRI) procedures may lead to significant increase in temperature and local specific absorption rate (SAR) for patients with implanted pacemaker (PM). In this paper two numerical models were developed to reproduce the heat generation process which occurs at the lead tip of an implanted PM when exposed to a RF field: the former (thermal model) shows how the position of temperature probes definitely affects the estimation of temperature rise and SAR value measured on the lead tip. The transversal contact between the active portion of the probe and the lead tip is the configuration associated with the highest estimation of temperature and SAR, whereas other configurations may lead to an underestimation close to 15% and 70% for temperature and SAR, respectively. The latter (RF model) predicted higher temperature increase and SAR value for right pectoral implants compared to left ones.

1. Introduction

Today, Magnetic Resonance Imaging (MRI) is contraindicated for patients implanted with pacemakers (PM) and implantable cardioverter defibrillators (ICD) [1]. Most of the publications [2,3] dealing with novel MR techniques on patients with implanted linear conductive structures, point out that the presence of these structures may produce an increase in the local absorption rate (SAR) and a temperature growth that may bring living tissues to necrosis and then to death.

The amount of heating has been investigated by several groups and temperature elevations observed spread from not significant values up to tens of degrees [4-6]. The lack of standardization in the positioning of temperature probes may partially explain such differences. In addition the large number of variables which may be involved in the amount of heat generation as well as the occurring of resonance phenomena make difficult to perform extensive and exhaustive experimental measures.

Aim of this paper is first to evaluate the error

associated with the estimation of temperature and SAR on a PM lead during MRI. To this aim, a first numerical model (thermal model) was developed to characterize the temperature and SAR field near a lead tip and to estimate the error made by fluoroptic probes in temperature and SAR measurement, due to their physical dimensions. Secondly, another numerical model (RF model) simulating the MRI coil, a human trunk and various PM implants was proposed, in order to investigate the effect of the implant geometry (left vs right pectoral implant) on temperature increase and SAR.

2. Methods

A. Thermal model

Aim of the thermal model was to estimate the maximum temperature increase and local SAR deposition around the lead tip, and to determine the measurement uncertainty due to probe positioning and physical dimensions.

A three-dimensional model was developed by using a finite-elements commercial software (FEMLAB 3.1, Comsol Multiphysics). This software allows to develop a coupled analysis that involved simultaneously both thermal and electromagnetic equations. The native 3-D drawing section of the software was used to represent a realistic geometry of the terminal portion of a PM lead (Fig. 1), in an external domain, consisting of a gelled saline-filled cylinder (radius: 5cm, height: 10cm).

Electromagnetic and thermal properties (density, heat capacity, thermal conductivity, electrical conductivity) of the different elements were chosen to most closely approximate those of human tissues and of a real PM lead. Since it is our interest to evaluate temperature field around the tip, we performed an electrostatic analysis, in which the model was excited by imposing a DC voltage gap between the active portion of the PM electrode and a boundary side of the external domain, set at a reference voltage. This excitation simplifies the complexity of the numerical model and thus allows a significant increase in the spatial resolution. We used the numerical model to evaluate the error associated with temperature increase and SAR measurement through fluoroptic probes around the tip of the lead. The error was quantified as follows:

$$\Delta T\% \text{ local error} = \frac{\Delta T_{\text{probe}} - \Delta T_{\text{probe max}}}{\Delta T_{\text{probe max}}}$$

$$\Delta T\% \text{ maximum error} = \frac{\Delta T_{\text{probe}} - \Delta T_{\text{max}}}{\Delta T_{\text{max}}}$$

$$\text{SAR}\% \text{ local error} = \frac{\text{SAR}_{\text{probe}} - \text{SAR}_{\text{probe max}}}{\text{SAR}_{\text{probe max}}}$$

$$\text{SAR}\% \text{ maximum error} = \frac{\text{SAR}_{\text{probe}} - \text{SAR}_{\text{max}}}{\text{SAR}_{\text{max}}}$$

where $\text{SAR}_{\text{probestmax}}$, $\text{SAR}_{\text{probe}}$, SAR_{max} are the value of SAR calculating as the dT/dt from the maximum temperature increase in the area covered by the probe ($\Delta T_{\text{probestmax}}$), from the average temperature rise in the same area (ΔT_{probe}) and from the maximum temperature increase in the whole domain (ΔT_{max}), respectively.

Temperature field was sampled in different points, simulating four different contact configurations between the lead tip and the fluoroptic probe (Fig. 1):

- Transversal contact;
- Tip-to-side contact;
- Tip-to-tip contact;
- Side-to-side contact;

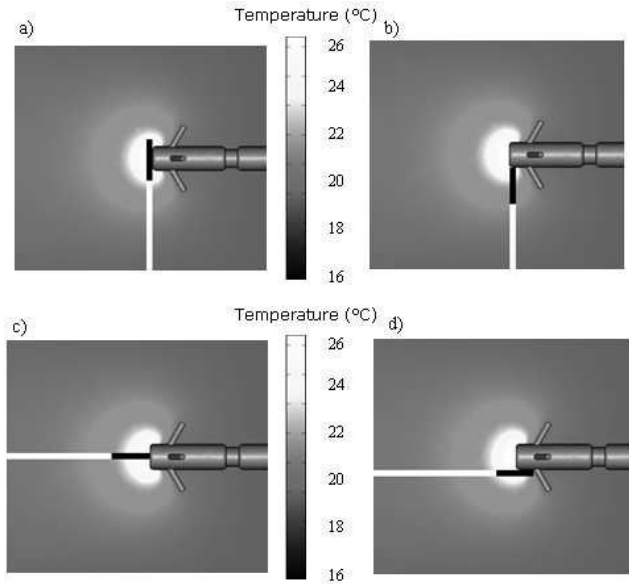


Figure 1: Temperature field resulting from the numerical model. The different contact configurations for the probes are also depicted: (a) transversal contact; (b) tip-to-side contact; (c) tip-to-tip contact; (d) side-to-side contact. Temperature gray-map is valid only for the gelled domain, but not for the probes and the lead.

B. RF model

The RF coil of a 1.5 T MRI system was modeled using a FDTD (*Finite Difference Time Domain*) commercial software (SEMCAD X, version 10.0, SPEAG, Zurich). The MR coil is a birdcage with 16 cylindrical copper ($\epsilon_r = 1$, $\sigma = 5.8 \cdot 10^7$ S/m) legs ($R_{\text{leg}} = 2$ cm, $H_{\text{leg}} = 63$ cm) uniformly distributed along a circumference ($R_{\text{cage}} = 34.5$ cm) and two end rings ($H_{\text{ring}} = 2$ cm). A current excitation has been imposed at the centre of the birdcage legs with sinusoidal time behavior and a phase delay equal to the azimuthal angle, so to obtain circular polarization. This corresponds to an increasing 22.5° phase shift between elements. This current is able to simulate the quadrature excitation, usually adopted in real birdcages.

The human trunk was represented as a parallelepiped box ($30 \times 20 \times 60$ cm³) whose electrical properties mimic the average ones of human tissues at the considered frequency ($\epsilon_r = 78.2$, $\sigma = 0.6$ S/m at 64 MHz). The amplitude of the current excitation was chosen so to have a mean SAR value in the trunk simulator of 1W/Kg.

Once characterized the electric and magnetic field distribution in the human trunk simulator, the effect of the presence of a PM and its lead on the power deposition at the tip was investigated. In particular, aim of the RF model was to evaluate the difference between a left and a right pectoral implant. A PM with its lead was then set in the box at a depth of 1 cm from the upper surface. The PM chassis was modeled as a titanium $40 \times 50 \times 0.6$ cm³ box and the lead as a 62 cm-long copper wire (radius = 0.4 mm) with a silicon insulation sheath (radius = 0.9 mm). Two typical implant configurations in the left and in the right pectoral region of the trunk simulator were reproduced and the SAR distribution was mapped in the two cases.

C. Experimental measures

The results of the numerical model were compare to several experimental measures preformed in a real 1.5 T MRI Scanner (Siemens Magnetom Sonata Maestro Class), using a human-shaped torso simulator realized at the Dept. of Technology and Health of the National Institute of Health in Rome. The simulator consists of a torso-shaped transparent PVC phantom of the size of a 70 kg male. Internal volume of the torso is 32 litres. A PVC grid is mounted inside the torso to support the PM, the PM lead, and the temperature probes. The torso was filled with a hydroxy-ethyl-cellulose (HEC) gel, which reproduces the electromagnetic proprieties of living tissues ($\epsilon_r = 78.2$, $\sigma = 0.6$ S/m). The temperature measurements were performed using a fluoroptic thermometer (Luxtron, Model 3100, Santa Clara, California), with accuracy of measurements of 0.1°C , operating at 8 samples per second. A transversal contact

between the active portion of the probe and the PM lead tip was chosen, so to get the highest estimation of temperature and SAR. The implant configurations investigated were the same reproduced in the RF model (right and left pectoral implant). The MRI parameters (TR, TE and Flip Angle) were adjusted to reach a whole-body SAR of 2 W/Kg estimated by the scanner.

3. Results

A. Thermal model

As illustrated in Fig. 1, the temperature gradient that arises around the lead tip is very high and thus the physical dimension of the fluoro-optic probes can not be neglected. The measure error is strictly related to the positioning of active portion of the probes, which is encapsulated inside a pigmented region that may cover areas with a great difference in temperature gradient.

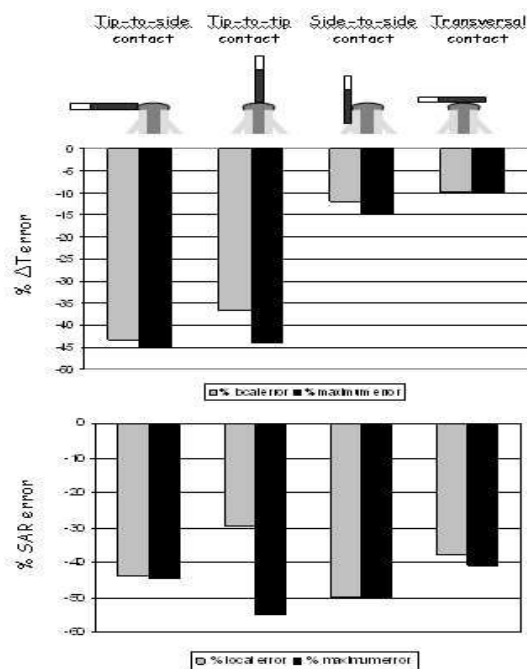


Figure 2: Underestimation resulting from the numerical model in temperature increase and SAR measurement made by fluoro-optic probes in different positions.

The values of the local and maximum percentage errors of temperature and SAR are reported in Fig. 2. The maximum error in the temperature increase measurement (percentage error: -44.9%, absolute error: -4°C) is associated to the tip-to-side contact configuration, while the lowest underestimation (transversal contact) resulted in a percentage error as low as -9.7% and in an absolute error as low as -0.88°C.

The errors associated to SAR measurement are

significantly higher than those of temperature (range -30% -50%). In addition, the positioning of the probes plays a minor role. The transversal contact is always the configuration associated to the lowest error (percentage error: -40.8%, absolute error: -1068.7 W/Kg), while tip-to-tip contact is characterized by the most homogeneous SAR field (lowest local error).

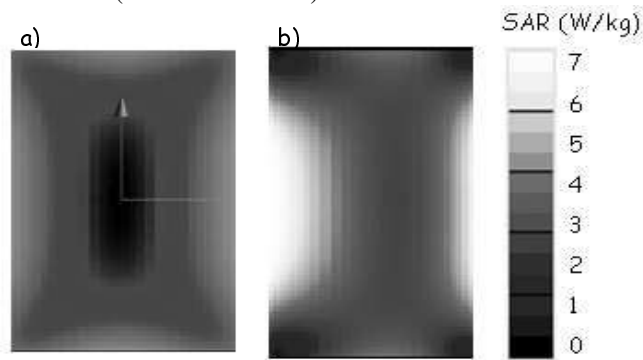


Figure 3: SAR field in the trunk simulator: a) coronal plane through the center of the coil; b) plane 1 cm below the thorax surface.

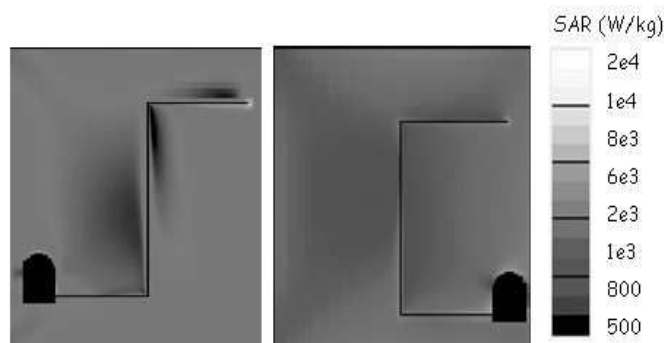


Figure 4: SAR field in the trunk simulator with a PM implanted: a) right implant; b) left implant.

B. RF model

First of all, the exposure of the thorax model, without the PM, to 60 W of input power at 64 MHz, has been studied. The E field and the H field in the trunk simulator show a symmetric distribution on the coronal plane through the center of the coil. This symmetry gets lost on a plane 1 cm below the thorax surface, corresponding to the section where the PM and the catheter will be placed. Since the SAR distribution is related to that of the electric field, it follows a distribution similar to that of the E field. Under these conditions a SAR_{PEAK} as averaged over a single voxel (0.5 mm^3) of 6.82 W/kg has been obtained, while the SAR_{WB} (mean SAR in the thorax simulator) is equal to 1.08 W/kg.

The effect of the implant of a PM on the SAR

distribution was then investigated. Fig. 4 shows how the presence of the lead determines high local SAR values: in particular, the left-pectoral configuration implant determines a SAR_{PEAK} of 1887 W/kg at the lead tip. The right-pectoral implant produces a significantly higher increase in the power deposition the left ones: a SAR_{PEAK} of 20670 W/kg at the lead tip was obtained.

C. Experimental measures

Experimental measures on the human-shaped phantom undergoing a real MRI examination confirmed what predicted by the RF model, even if the difference between the two implant configurations is less marked. The right pectoral implant produced a temperature increase up to 9.41°C and a local SAR value at the lead tip of 2871 W/kg; temperature increase and SAR decrease at 6.92°C and 2214 W/kg for the left pectoral implant.

4. Discussion and conclusions

The large number of variables which may be involved in the amount of heat generation as well as the occurring of resonance phenomena make difficult to perform extensive and exhaustive experimental measures. For this reason, the development of numerical models represents a very useful approach to investigate the potential effects of MRI on PMs, ICDs and other active implantable medical devices (AIMDs). Temperature field computed in the thermal model points out how the temperature gradient which arises around the lead tip is so high that the physical dimensions of the probes can not be neglected. As a consequence, the measure of the temperature increase is affected by an underestimation of 9.7% in the best case (transversal contact) and of 44.9% in the worst one (tip-to-side contact), respect the maximum temperature in the whole domain. The error associated to evaluation of local SAR is higher than the temperature one: SAR is calculated as the slope of the initial linear temperature increase and thus is affected by the spatial distribution of the temperature in the first instants of the heat generation process. Thus, the effect of physical probe dimensions is higher than at steady state. After a 300s periods the temperature field has become more homogenous and the related error has consequently decreased. In addition, the underestimation of the SAR is less sensitive to the probe positioning than temperature measures. SAR is underestimated of about 40% for the transversal contact configuration, and about 55% in the tip-to-tip contact. The FDTD birdcage model well simulates the electromagnetic field generated by an actual RF coil of a MR system. The E field resulting from the RF model, if not calculated on a plane through the center of the coil, shows an asymmetric distribution. For a plane 1 cm below the thorax surface, where a PM is typically placed, the electric field reaches the highest values in the

right-half region of the trunk simulator. This fact may justify, at least partially, the significant difference in power deposition between a left and a right pectoral implant. Experimental measures substantially confirmed the results of the numerical model: temperature and SAR measures performed on the human-shaped phantom reveal the importance of the implant geometry in the amount of heat generation. In agreement with the numerical results, a right implant produces a higher power deposition than the left one. However, this gap is less marked than the one resulting from the numerical model. This means that there are several elements that influence the heat generation process and that are still not well simulated by the model.

References

- [1] Kanal E, Borgstede JP, Barkovich AJ, Bell C, Bradley WG, Etheridge S, Felmlee JP, Froelich JW, Hayden J, Kaminski EM, Lester JW Jr, Scoumis EA, Zaremba LA, Zininger MD. 2002. American College of Radiology white paper on MR-safety. *AJR Am J Roentgenol.*; 178: 1335–1347.
- [2] Shellock FG, Crues JV III. 2002. MR-safety and the American College of Radiology white paper. *AJR Am J Roentgenol.*; 178:1349–1352.
- [3] Baker KB, Tkach JA, Nyenhuis JA, Phillips M, Shellock FG, Gonzalez-Martinez J, Rezai AR. 2004. Evaluation of Specific Absorption Rate as a Dosimeter of MRI-Related Implant Heating. *Journal of Magnetic Resonance Imaging* 20 315–320.
- [4] Achenbach S, Moshage W, Diem B, Bieberle T, Schibgilla V, Bachmann K. 1997. Effects of magnetic resonance imaging on cardiac pacemakers and electrodes, *Am Heart J.* 134 467–473.
- [5] Sommer T, Vahlhaus C, Lauck G, von Smekal A, Reinke M, Hofer U, Block W, Traber F, Schneider C, Gieseke J, Jung W, Schild H. 2000. MR imaging and cardiac pacemakers: in-vitro evaluation and in-vivo studies in 51 patients at 0.5 T, *Radiology* 215 869–879.
- [6] Roguin A, Zviman MM, Meininger GR, Rodrigues ER, Dickfeld TM, Bluemke DA, Lardo A, Berger RD, Calkins H, Halperin, HR. 2004. Modern Pacemaker and Implantable Cardioverter/Defibrillator Systems Can Be Magnetic Resonance Imaging Safe. In Vitro and In Vivo Assessment of Safety and Function at 1.5 T, *Circulation* 110 475-482.

Address for correspondence

Eugenio Mattei
 Dept. of Technologies and Health
 Istituto Superiore di Sanità
 Viale Regina Elena 299
 00161 Roma, Italy
 Tel. +390649902028
 eugmattei@hotmail.com